Dyes and Pigments 121 (2015) 79–87

Contents lists available at ScienceDirect

Dyes and Pigments

journal homepage: www.elsevier.com/locate/dyepig

# Highly efficient benzodifuran based ruthenium sensitizers for thin-film dye-sensitized solar cells

Mariusz J. Bosiak [a, *], Marcin Rakowiecki [a], Andrzej Wolan [a], Jolanta Szlachta [b], Edyta Stanek [b], Dawid Cycoń [b], Krzysztof Skupień [c]

[a] Synthex Technologies Sp. z o.o., Gagarina 7, 87-100 Toruń, Poland
[b] ML System Sp. z o. o., Warszawska 50 d, 35-230 Rzeszów, Poland
[c] 3D-nano, Powstańców 64b, 31-670 Cracow, Poland

ARTICLE INFO

*Article history:*
Received 21 March 2015
Accepted 11 May 2015
Available online 19 May 2015

*Keywords:*
DSSC
Benzodifuran
The Sonogashira reaction
Ruthenium dyes
Solar cells
Benzofuran

ABSTRACT

The synthesis of 4,4′-dibenzodifuran-2,2′-bipyridine derivatives as ligands of organic ruthenium dyes for DSSC applications is described. Two new heteroleptic ruthenium complexes have been prepared and compared with commercially available **N719** and **Z907** dyes, using dip dyeing and flow dyeing methods in large area testing cells prepared for industrial purposes. The newly synthesized dyes revealed higher solar-to-electric energy conversion efficiency ($\eta$), measured at the AM1.5G conditions, up to 21% compared to **N719** and up to 46% compared to **Z907**, and external quantum efficiency of 53%. These results can be explained by enhanced light-harvesting of the benzodifuran moiety of the dyes that is related to photocurrent.



## 1. Introduction

Since 1991 when O'Regan and Grätzel [1] described the first dye-sensitized solar cell (DSSC) containing ruthenium dye as a photosensitizer, this technology have attracted tremendous interest due to its low manufacturing cost, a remarkable stability, and respectable high solar-to-electric energy conversion efficiency ($\eta$) up to 12% [2]. Although the perovskite type sensitizers derived from lead halides and applied by spin coating technique allowed to reach the efficiency of ~19.3% [3], there is still place for organic ruthenium dyes soluble in "green" organic solvents, such as ethanol, and easily applicable by "dip coating" or "flow dyeing" techniques, well suited for the preparation of large area solar panels.

The first commonly used homoleptic ruthenium complexes for DSSC applications (**N3** and **N719**) developed in Grätzel group [4,5] revealed $\eta$~11% for devices based on these dyes under one-sun illumination (Fig. 3) [6,7] The main drawback of the devices was their low stability. To improve their durability an amphiphilic ruthenium sensitizer **Z907** was developed by replacing one 4,4′-dicarboxylic-2,2′-bipyridine (dcbpy) ligand in the **N3** dye with an ancillary 4,4′-dinonyl-2,2′-bipyridine ligand [8–10]. Although stability of the device based on **Z907** improved significantly, the efficiency decreased, mainly due to lower light-harvesting, related to the molar extinction coefficient for two UV–Vis absorption bands – at 350–450 nm (ligand-centered charge transfer (LCCT) transitions ($\pi$ - $\pi^*$)), as well as at 500–600 nm (metal-to-ligand charge transfer (MLCT) transitions (4d - $\pi^*$)). To improve the light-harvesting efficiency via an enhanced molar extinction coefficient, many heteroleptic ruthenium complexes derived from 2,2′-bipyridine substituted with aryl, heteroaryl and aryl-vinyl groups were developed [11–25]. Herein, the synthesis and photovoltaic characterization of benzodifuran (**BDF**) derived ruthenium dyes of high energy conversion efficiency is described.

## 2. Experimental

### 2.1. Materials and general methods

Experiments with air and moisture sensitive materials were carried under argon atmosphere. Glassware was oven dried for several hours, assembled hot, and cooled in a stream of argon. Silica gel 60, Merck 230–400 mesh, was used for preparative column flash chromatography. Analytical TLC was performed using Sigma–Aldrich silica gel on TLC Al foils with fluorescent indicator

* Corresponding author. Tel.: +48 512038649; fax: +48 56 6542477.
*E-mail address:* bosiak@synthex.com.pl (M.J. Bosiak).

http://dx.doi.org/10.1016/j.dyepig.2015.05.013
0143-7208/

254 nm, 0.2 mm plates. 1-Octanol, iodine, morpholine, 4,4′-dibromo-2,2′-bipyridine, [1,1′-bis(diphenylphosphino)ferrocene] dichloropalladium(II), copper iodide, diisopropylamine, ethynyltrimethylsilane, 1M tetrabutylammonium fluoride solution in THF, dichloro(*p*-cymene)ruthenium(II) dimer, 2,2′-bipyridine-4,4′-dicarboxylic acid, ammonium thiocyanate, and tetrabutylammonium hydroxide were commercially available from Sigma–Aldrich, Merck or Fluorochem, and were used without further purification. [2,2′-Bipyridine]-4,4′-dicarbaldehyde was prepared according to the literature procedure [26]. Solvents were purchased from Avantor and Sigma–Aldrich. Toluene was distilled from sodium benzophenone ketyl prior to use, DMF was stirred overnight with calcium hydride, filtered, distilled at 20 mmHg, and stored over 4A molecular sieves. Chloroform, diethyl ether, methanol, anhydrous ethanol, THF, *n*-heptane, and ethyl acetate were used without further purification. Deuterated solvents for NMR spectroscopy were purchased from Sigma–Aldrich. Sephadex LH-20 was purchased from GE Healthcare. **N719** and **Z907** dyes were purchased from Dyesol. Melting points were determined with a Büchi SMP 32 and Barnstead-Thermolyne Mel-Temp II apparatus in open capillaries and are uncorrected. Elemental analyses were performed at Elementary Analysensysteme GmbH Vario MACRO CHN analyzer.

#### 2.1.1. Spectroscopic measurements

$^1$H and $^{13}$C NMR spectra were recorded on a Bruker Advance III 400 MHz or Bruker Advance III 700 MHz instrument at ambient temperature. Chemical shifts are reported in parts per million ($\delta$ scale), coupling constants ($J$ values) are listed in Hertz. Anhydrous ethanol (spectrometric grade from Sigma–Aldrich) was employed as solvent for absorption measurements. UV/Vis absorption spectra of dyes solutions and sensitized $TiO_2$ films were recorded by means of a Jasco V670 UV–Vis–NIR spectrophotometer equipped with liquid a cell holder (10 mm quartz cell, versus solvent blank) and thin film holder. IR spectra were recorded on a Perkin Elmer FT-IR Spectrum Two spectrometer equipped in diamant ATR.

### 2.2. Synthesis of the compounds

#### 2.2.1. Ethyl 5-hydroxy-2-methylbenzofuran-3-carboxylate (**1**)

A solution of *p*-benzoquinone (54.045 g, 0.5 mol) and ethyl acetoacetate (200 mL, 1.583 mol) in dry acetone (200 mL) was added dropwise during 9 h to a mechanically stirred solution of anhydrous zinc chloride (70 g, 0.513 mol) in acetone (100 mL) and acetic acid (5 mL) at 75 °C. The mixture was stirred for additional 10 min, transferred into a large crystallizer and left opened in fume cupboard overnight. The crystallizer was transferred into freezer and left for 24 h. Precipitate was filtered off, washed with cold MeOH (2 × 50 mL) and dried on air. Crude product was crystallized from toluene to give 47.50 g (43%) of white solid, mp = 143–144 °C. Lit [27]. 143.5–144 °C. $^1$H NMR (700 MHz, $CDCl_3$); $\delta$ ppm: 1.41 (t, $J$ = 7 Hz, 3H, $CH_3$), 2.71 (s, 3H, $CH_3$), 4.38 (q, $J$ = 7 Hz, 2H, CH), 6.79–6.80 (dd, $J$ = 9.1 Hz, $J$ = 2.8 Hz, 2H, $CH_2$), 5.88 (s, 1H, CH), 7.24 (d, $J$ = 4.2 Hz, 1H, CH), 7.26 (s, 1H, CH), 7.48 (d, $J$ = 2.8, 1H, CH). $^{13}$C NMR ($CDCl_3$, 175 MHz); $\delta$ ppm: 15.38 ($CH_3$), 15.75 ($CH_3$), 61.53 ($CH_2$), 107.84 (CH), 109.86 (C), 112.25 (CH), 113.72 (CH), 128.26 (C), 149.52 (C), 153.67 (C), 165.52 (C), 165.86 (C). IR (ATR) $\nu_{max}$ cm$^{-1}$: 3323, 1668, 1623, 1607, 1580, 1475, 1464, 1417, 1382, 1348, 1300, 1259, 1217, 1168, 1111, 1087, 1027, 954, 866, 853, 838, 809, 784, 736, 682, 652, 617, 573. Anal. Calcd. for $C_{12}H_{12}O_4$: C, 65.45; H, 5.49. Found: C, 65.61; H, 5.44.

#### 2.2.2. Octyl 5-hydroxy-2-methylbenzofuran-3-carboxylate (**2**)

To a dispersion of ethyl 5-hydroxy-2-methylbenzofuran-3-carboxylate (29.54 g, 134 mmol) in 1-octanol (300 mL), concentrated sulfuric acid (1 mL) was added and the mixture was heated to 150 °C in opened flask and stirred at this temperature for 18 h. It was poured into concentrated solution of sodium bicarbonate (200 mL) and brine (100 mL), stirred for several minutes and extracted with ethyl acetate (3 × 100 mL). Combined organic layers were dried with anhydrous magnesium sulfate. The ethyl acetate was removed using rotary evaporator and the remaining 1-octanol was distilled off under reduced pressure. To a slurry *n*-heptane (500 mL) was added, the mixture was heated to reflux and filtered through a warm Büchner funnel. The filtrate was cooled overnight and the flaky precipitate was filtered off and dried to obtain 32.87 g (80%) of pure solid, mp 93–94 °C. $^1$H NMR ($CDCl_3$, 400 MHz); $\delta$ ppm: 0.90 (t, $J$ = 6.8 Hz, 3H, $CH_3$), 1.28–1.42 (m, 8H, $4CH_2$), 1.45–1.52 (m, 2H, $CH_2$), 1.78–1.86 (m, 2H, $CH_2$), 2.76 (s, 3H, $CH_3$), 4.36 (t, $J$ = 6.8 Hz, 2H, $CH_2$), 5.23 (s, 1H, OH), 6.82 (dd, $J$ = 8.8 Hz, $J$ = 2.6 Hz, 1H, $CH_{Ar}$), 7.30 (d, $J$ = 8.8 Hz, 1H, $CH_{Ar}$), 7.46 (m, 1H, $CH_{Ar}$). $^{13}$C NMR ($CDCl_3$, 100 MHz); $\delta$ ppm: 14.07 ($CH_3$), 14.81 ($CH_3$), 22.63 ($CH_2$), 26.10 ($CH_2$), 28.73 ($CH_2$), 29.19 ($CH_2$), 29.22 ($CH_2$), 31.78 ($CH_2$), 64.82 ($CH_2$), 106.81 (CH), 108.90 (C), 111.25 (CH), 112.79 (CH), 127.31 (C), 148.50 (C), 152.85 (C), 164.38 (C), 165.07 (C). IR (ATR) $\nu_{max}$ cm$^{-1}$: 3348, 2948, 2923, 2854, 1670, 1622, 1605, 1577, 1463, 1415, 1394, 1382, 1359, 1298, 1268, 1258, 1212, 1173, 1111, 1094, 1020, 962, 944, 863, 837, 806, 789, 783, 735, 724, 648, 619, 611, 581. Anal. Calcd. for $C_{18}H_{24}O_4$: C, 71.03; H, 7.95. Found: C, 71.21; H, 7.97.

#### 2.2.3. Ethyl 5-hydroxy-6-iodo-2-methylbenzofuran-3-carboxylate (**3**)

Ethyl 5-hydroxy-2-methylbenzofuran-3-carboxylate (**1**) (26.43 g, 120 mmol) and iodine (48.72 g, 192 mmol, 1.6 equiv.) were dispersed in anhydrous methanol (100 mL) and stirred for 5 min under argon. The mixture was cooled to 0 °C, and morpholine (30.32 g, 348 mmol, 2.9 equiv.) was added dropwise at a rate to keep the temperature below 30 °C, slowly heated to 35 °C, and stirred at this temperature for 120 h. Water (20 mL) was added and the mixture was left at −20 °C overnight. Precipitate was filtered off, washed with cold methanol of (−25 °C, 3 × 60 mL), and dried to obtain 46.91 g of beige solid. It was extracted with diethyl ether (450 mL) using a Soxhlet extractor for 48 h. The crude product was finally crystallized from methanol to obtain 13.97 g (34%) of pure white solid, mp = 196–197 °C. Lit [27]. 194–194.5 °C. $^1$H NMR ($CDCl_3$, 700 MHz); $\delta$ ppm: 1.44 (t, $J$ = 7.2 Hz, 3H, $CH_3$), 2.73 (s, 3H, $CH_3$), 4.40 (q, $J$ = 7.2 Hz, 2H, $CH_2$), 5.28 (s, 1H, OH), 7.56 (s, 1H, $CH_{Ar}$), 7.73 (s, 1H, $CH_{Ar}$). $^{13}$C NMR ($CDCl_3$, 100 MHz); $\delta$ ppm: 14.42 ($CH_3$), 14.56 ($CH_3$), 60.47 ($CH_2$), 80.68 (C), 106.25 (CH), 108.98 (C), 119.63 (CH), 128.38 (C), 148.73 (C), 151.25 (C), 164.11 (C), 165.11 (C). IR (ATR) $\nu_{max}$ cm$^{-1}$: 3255, 1672, 1614, 1582, 1447, 1405, 1380, 1345, 1279, 1268, 1183, 1166, 1150, 1115, 1093, 1033, 964, 909, 862, 841, 800, 786, 722, 657, 590. Anal. Calcd. for $C_{12}H_{11}IO_4$: C, 41.64; H, 3.20. Found: C, 41.48; H, 3.21.

#### 2.2.4. Octyl 5-hydroxy-6-iodo-2-methylbenzofuran-3-carboxylate (**4**)

Octyl 5-hydroxy-2-methylbenzofuran-3-carboxylate (**2**) (12.16 g, 40 mmol) and iodine (24.38 g, 96 mmol, 2.4 equiv.) were dispersed in anhydrous methanol (60 mL) and stirred for 10 min under argon. The mixture was cooled to 0 °C and morpholine (15.20 mL, 175 mmol, 4.35 equiv.) was added dropwise at a rate to keep the temperature below 30 °C, slowly heated to 35 °C, and stirred at this temperature for 48 h. Water (12 mL) was added and the mixture was left at −20 °C overnight. Precipitate was filtered off, washed with cold methanol (−25 °C, 5 × 25 mL) and dried to obtain 17.10 g of beige solid. It was dispersed in chloroform (300 mL) and stirred for 5 min. Insoluble precipitate of morpholine hydroiodide was filtered off and the filtrate was concentrated to obtain 10.02 g of crude brown product. Crystallization from methanol/water (200 mL/25 mL) gave 8.89 g (52%) of light yellow

solid, mp = 124–125 °C. $^1$H NMR ($CDCl_3$, 700 MHz); δ ppm: 0.90 (t, $J$ = 6.8 Hz, 3H, $CH_3$), 1.26–1.42 (m, 8H, $4CH_2$), 1.44–1.51 (m, 2H, $CH_2$), 1.78–1.86 (m, 2H, $CH_2$), 2.75 (s, 3H, $CH_3$), 4.36 (t, $J$ = 6.8 Hz, 2H, $CH_2$), 5.44 (s, 1H, OH), 7.59 (s, 1H, $CH_{Ar}$), 7.74 (s, 1H, $CH_{Ar}$). $^{13}$C NMR (DMSO-$d_6$, 175 MHz); δ ppm: 14.01 ($CH_3$), 14.36 ($CH_3$), 22.14 ($CH_2$), 25.59 ($CH_2$), 28.23 ($CH_2$), 28.67 ($CH_2$), 28.69 ($CH_2$), 31.23 ($CH_2$), 64.17 ($CH_2$), 80.95 (C), 105.15 (CH), 108.12 (C), 120.34 (CH), 127.04 (C), 147.63 (C), 153.25 (C), 163.38 (C), 164.22 (C). IR (ATR) $\nu_{max}$ cm$^{-1}$: 3266, 2959, 2918, 2854, 1669, 1610, 1580, 1467, 1448, 1400, 1355, 1340, 1262, 1201, 1184, 1166, 1152, 1099, 1021, 962, 887, 865, 840, 789, 726, 676, 661, 593, 558, 474. Anal. Calcd. for $C_{18}H_{23}IO_4$: C, 50.24; H, 5.39. Found: C, 50.53; H, 5.41.

### 2.2.5. Diethyl 6,6′-([2,2′-bipyridine]-4,4′-diyl)bis(2-methylbenzo[1,2-b:4,5-b′]difuran-3-carboxylate) (**6a**)

4,4′-Dibromo-2,2′-bipyridine (1.5699 g, 5 mmol), [1,1′-bis(diphenylphosphino)ferrocene]dichloropalladium(II) (0.3660 g, 0.5 mmol, 10% mol), and copper iodide (0.0952 g, 0.5 mmol, 10% mol) were placed under argon in a Schlenk flask and dry toluene (20 mL) was added, followed by diisopropylamine (10 mL, 70 mmol). The mixture was stirred for 15 min and ethynyltrimethylsilane (1.2766 g, 13 mmol) in dry toluene (5 mL) was added in one portion. The mixture was heated to 80 °C until all ethynyltrimethylsilane was consumed, as judged by GC (1.5 h). It was cooled to rt and 1M tetrabutylammonium fluoride solution in THF (10 mL) was added. After 1 min ethyl 5-hydroxy-6-iodo-2-methylbenzofuran-3-carboxylate (3.4630 g, 10 mmol) in dry toluene (50 mL) was added and the mixture was heated to 80 °C for 20 h. It was cooled to rt, water (40 mL) was added and filtered using Büchner funnel. Precipitate was returned to the flask, water (50 mL) and diethyl ether (50 mL) were added and stirred for 30 min. The procedure was repeated using methanol (120 mL) and finally THF (120 mL). The precipitate was filtered using Büchner funnel and dried under vacuum to give 2.5070 g (78%) of pure desired product, mp > 300 °C. 1H NMR ($CDCl_3$, 700 MHz); δ ppm: 1.53 (t, $J$ = 7.1 Hz, 6H, 2 × $CH_3$), 2.82 (s, 6H, 2 × $CH_3$), 4.48 (q, $J$ = 7.1 Hz, 4H, 2 × $CH_2$), 7.47 (s, 2H, 2 × $CH_{Ar}$), 7.63 (s, 2H, 2 × $CH_{Ar}$), 7.81 (s, 2H, 2 × $CH_{Ar}$), 8.11 (s, 2H, 2 × $CH_{Ar}$), 8.83 (s, 2H, 2 × $CH_{Ar}$), 8.91 (s, 2H, 2 × $CH_{Ar}$). Solubility too low for $^{13}$C NMR. IR (ATR) $\nu_{max}$ cm$^{-1}$: 2979, 1709, 1601, 1368, 1174, 1157, 1081, 853, 832, 809, 701, 533. Anal. Calcd. for $C_{38}H_{28}N_2O_8$: C, 71.24; H, 4.41; N, 4.37. Found: C, 71.40; H, 4.38; N, 4.39.

### 2.2.6. Dioctyl 6,6′-([2,2′-bipyridine]-4,4′-diyl)bis(2-methylbenzo[1,2-b:4,5-b′]difuran-3-carboxylate) (**6b**)

4,4′-Dibromo-2,2′-bipyridine (1.5699 g, 5 mmol), [1,1′-bis(diphenylphosphino)ferrocene]dichloropalladium(II) (0.3660 g, 0.5 mmol, 10% mol), and copper iodide (0.0952 g, 0.5 mmol, 10% mol) were placed under argon in a Schlenk flask and dry toluene (20 mL) was added followed by diisopropylamine (10 mL, 70 mmol). The mixture was stirred for 15 min and ethynyltrimethylsilane (1.2766 g, 13 mmol) in dry toluene (5 mL) was added in one portion. The mixture was heated to 80 °C until all ethynyltrimethylsilane was consumed as judged by GC (2 h). It was cooled to rt and 1M tetrabutylammonium fluoride solution in THF (13 mL) was added. After 1 min octyl 5-hydroxy-6-iodo-2-methylbenzofuran-3-carboxylate (4.3040 g, 10 mmol) in dry toluene (50 mL) was added and the mixture was heated to 80 °C for 14 h. It was cooled to rt, water (40 mL) was added and filtered using Büchner funnel. Precipitate was returned to the flask, water (50 mL) and diethyl ether (50 mL) were added and stirred for 10 min. The precipitate was filtered off and dried under vacuum, 3.8870 g (96%) of pure desired product, mp = 212–214 °C. 1H NMR ($CDCl_3$, 700 MHz); δ ppm: 0.89 (t, $J$ = 7.0 Hz, 6H, 2 × $CH_3$), 1.28–1.35 (m, 8H, 4 × $CH_2$), 1.36–1.39 (m, 4H, 2 × $CH_2$), 1.41–1.45 (m, 4H, 2 × $CH_2$), 1.51–1.55 (m, 4H, 2 × $CH_2$), 1.87–1.91 (m, 4H, 2 × $CH_2$), 2.82 (s, 6H, 2 × $CH_3$), 4.41 (t, $J$=7.0 Hz, 4H, 2 × $CH_2$), 7.46 (s, 2H, 2 × $CH_{Ar}$), 7.62 (s, 2H, 2 × $CH_{Ar}$), 7.80 (dd, $J$ = 5.0 Hz, $J$ = 1.5 Hz, 2H, 2 × $CH_{Ar}$), 8.10 (s, 2H, 2 × $CH_{Ar}$), 8.82 (d, $J$ = 5.0 Hz, 2H, 2 × $CH_{Ar}$), 8.90 (s, 2H, 2 × $CH_{Ar}$). Solubility too low for $^{13}$C NMR. IR (ATR) $\nu_{max}$ cm$^{-1}$: 2928, 2861, 1708, 1605, 1592, 1406, 1383, 1368, 1239, 1222, 1176, 1151, 1117, 1091, 1043, 988, 923, 863, 832, 808, 796, 701. Anal. Calcd. for $C_{50}H_{52}N_2O_8$: C, 74.24; H, 6.48; N, 3.46. Found: C, 74.43; H, 6.50; N, 3.49.

### 2.2.7. (TBA(Ru[(4-carboxylic acid-4′-carboxylate-2,2′-bipyridine)(Ligand-**6a**)(NCS)$_2$])) (***M44***)

A mixture of dichloro(*p*-cymene)ruthenium(II) dimer (0.3062 g, 0.5 mmol) and **6a** (0,6402 g, 1 mmol) in dry DMF (40 mL) was stirred in the dark, under argon at 150 °C, monitoring the disappearance of substrates and appearance of product by UV–Vis spectrometry (~2 h). 2,2′-Bipyridine-4,4′-dicarboxylic acid (0.2442 g, 1 mmol) was added and the mixture was stirred at 150 °C for 4 h. Ammonium thiocyanate (2.74 g, 36.5 mmol) was added and the mixture was stirred at 150 °C for another 4 h. It was cooled to rt, filtered, and DMF was removed with the rotary evaporator. To the residual slurry water (100 mL) was added and filtered. Precipitate was washed with water (100 mL) and dried under vacuum. The crude product was dissolved in DMF and then passed through a Sephadex LH-20 column with DMF as eluent. The main band was collected and concentrated. This purification process was repeated three times. Pure complex was dispersed in ethanol and titrated with 0.5M tetrabutylammonium hydroxide solution to pH = 9, stirred for 5 min, filtered, and the filtrate was titrated with 0.01M $HNO_3$ to pH = 5.2. Solvents were removed with the rotary evaporator, the product was washed with acidified water (pH = 5.2), and dried under vacuum and $P_2O_5$ to obtain 0.4966 g (36%) of pure complex as black plates, mp > 300 °C. IR-ATR, cm$^{-1}$: 2962, 2935, 2856, 2100, 1707, 1611, 1467, 1426, 1402, 1362, 1305, 1235, 1176, 1083, 1019, 979, 921, 853, 807, 782, 705, 473. Anal. Calcd. for $C_{52}H_{35}N_6O_{12}RuS_2{\cdot}TBA{\cdot}2H_2O$: C, 59.20; H, 5.48; N, 7.11. Found: C, 59.41; H, 5.52; N, 7.16.

### 2.2.8. (TBA(Ru[(4-carboxylic acid-4′-carboxylate-2,2′-bipyridine)(Ligand-**6b**)(NCS)$_2$])) (***M43***)

A mixture of dichloro(*p*-cymene)ruthenium(II) dimer (0.3062 g, 0.5 mmol) and **6a** (0.809 g, 1 mmol) in dry DMF (40 mL) was stirred in the dark, under argon at 150 °C, monitoring the disappearance of substrates and appearance of product by UV–Vis spectrometry (~2 h). 2,2′-Bipyridine-4,4′-dicarboxylic acid (0.2442 g, 1 mmol) was added and the mixture was stirred at 150 °C for 4 h. Ammonium thiocyanate (2.74 g, 36.5 mmol) was added and the mixture was stirred at 150 °C for another 4 h. It was cooled to rt, filtered, and DMF was removed with the rotary evaporator. To the residual slurry water (100 mL) was added and filtered. Precipitate was washed with water (100 mL) and dried under vacuum. The crude product was dissolved in DMF and then passed through a Sephadex LH-20 column with DMF as eluent. The main band was collected and concentrated. This purification was repeated three times. Pure complex was dispersed in ethanol and titrated with 0.5M tetrabutylammonium hydroxide solution to pH = 9. It was stirred for 5 min, filtered and the filtrate was titrated with 0.01M $HNO_3$ to pH = 5.2. Solvents were removed with the rotary evaporator, the product was washed with acidified water (pH = 5.2), and dried under vacuum and $P_2O_5$ to obtain 0.5418 g (35%) of black plates, mp > 300 °C. IR-ATR, cm-1: 2962, 2935, 2856, 2100, 1707, 1611, 1467, 1426, 1402, 1362, 1305, 1235, 1176, 1083, 1019, 979, 921, 853, 807, 782, 705, 473. Anal. Calcd. for $C_{64}H_{59}N_6O_{12}RuS_2{\cdot}TBA{\cdot}2H_2O$: C, 62.08; H, 6.45; N, 6.33. Found: C, 61.98; H, 6.42; N, 6.37.

The NMR spectra of the dyes are complex because they contain mixture of two diastereoisomers. As a result, the NMR spectra exhibit groups of broad peaks in the 6–9 ppm region that cannot be separated and unambiguously assigned, and have not been described.

### 2.3. Device fabrication

Fluorine-doped $SnO_2$ (FTO) glass plates (AGC ANS10ME, thickness 3.2 mm, 10 Ω/sq) with dimensions 200 × 70 mm were structured by means of ytterbium laser in order to obtain eight separated areas on photoanode and counter electrode. Then two holes (Ø1 mm) were drilled in counter electrode. After that glass plates were washed in ultrasonic bath containing de-ionized water, acetone and ethanol. A transparent single layer of 20-nm sized $TiO_2$ particles (18NR-T, Dyesol) and silver stripes (AG 7500-80, Johnson Matthey) were screen-printed on photoanode. A nanocolloidal Pt (3D-nano) layer and silver stripes were applied on counter electrode in the same way. All layers thickness was precisely determined using optical profiler (Sensofar PLU Neox), and the fabricated $TiO_2$ film thickness was around 5 μm (Fig. 1). Finally, the plates were dried at 150 °C for 30 min and annealed at 480 °C for 45 min. Dyeing process was conducted using dip dyeing and flow dyeing methods. In dip dyeing process photoanodes were immersed in solutions containing $1 \times 10^{-4}$ M dyes (**M43**, **M44**, **N719**, **Z907**) in ethanol for 24 h at room temperature. After dyeing the plates were rinsed with pure ethanol and dried under nitrogen. The dye-coated $TiO_2$ electrodes and Pt counter electrodes were assembled into a sealed sandwich-type cell by heating with a hot-melt ionomer film (Surlyn 1702, 25 μm thickness, DuPont) as a spacer between the electrodes. An encapsulation process was performed at 110 °C. The cell internal space was filled with a liquid electrolyte (EL-HPE, Dyesol) using the holes on the counter electrode, which were sealed by heating with a Surlyn sheet and a thin glass cover. The flow dyeing procedure was conducted after electrodes encapsulation. The same dyes solutions were flown through the cell for 8 h using peristaltic pomp and electrolyte-injecting holes. The obtained DSSC devices consists of eight 8 individual cells (Fig. 2), active area of single cell was 5 $cm^2$. In order to assure reliable results, six DSSC devices for each dye were prepared, where three of them were used in dip dyeing and next three in flow dyeing method.

### 2.4. Photovoltaic measurements

The DSSC devices were evaluated under 100 $mW/cm^2$ standard air mass 1.5 global (AM 1.5G) sunlight simulation with a class AAA solar cell analyzer (Model No. #SS150AAA, PV Test Solutions) conjugated with Keithley model 2401 digital source meter. A silicon solar cell fitted with a KG3 filter tested and certified by Fraunhofer ISE was used for calibration. The KG3 filter accounts for the

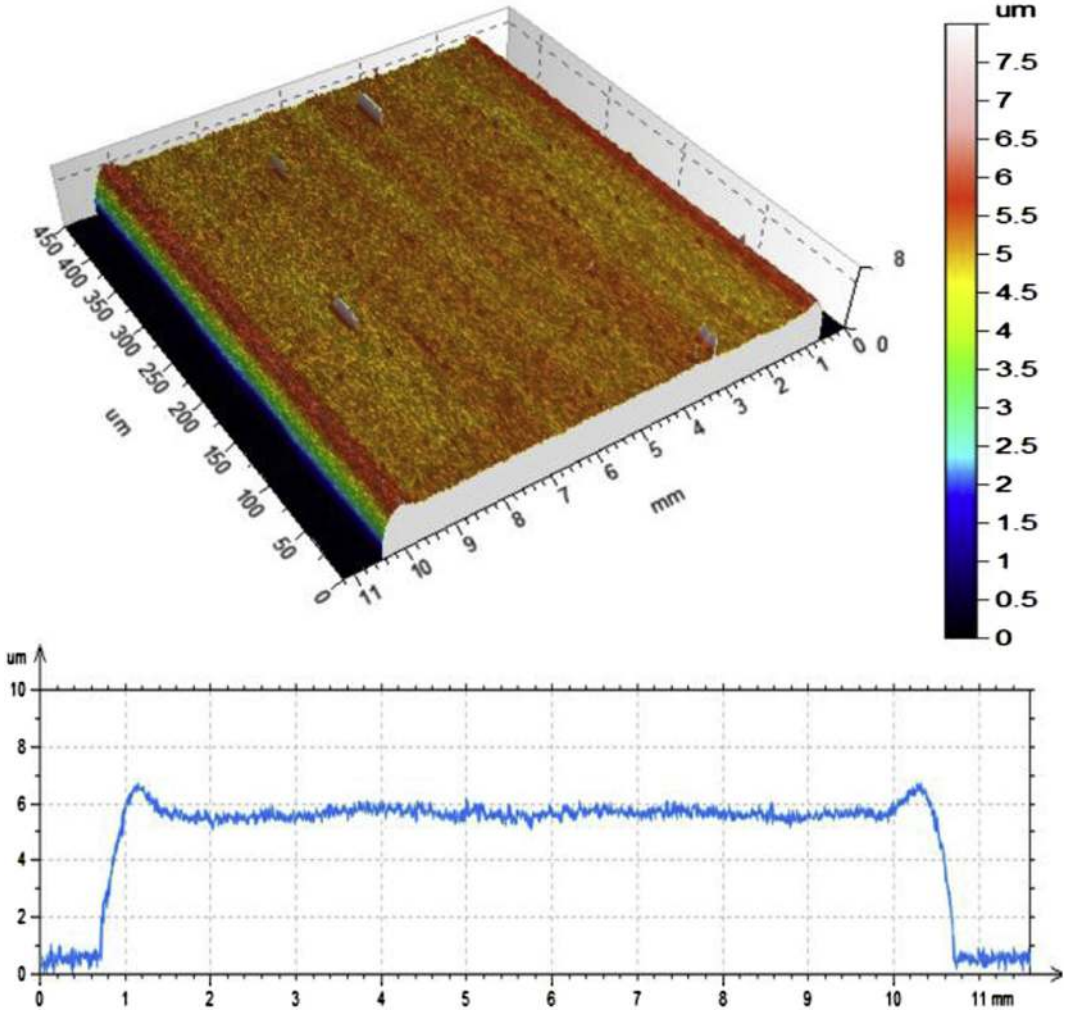


**Fig. 1.** Topography and profile of nanocrystalline $TiO_2$ layer deposited on photoelectrode.

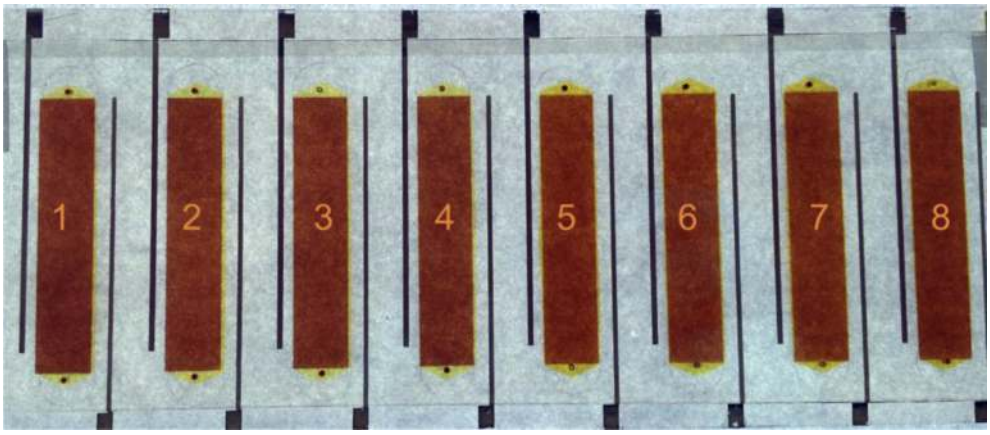


**Fig. 2.** Test plate with eight cells (**M43** dye) prepared in ML System Laboratory.

different light absorption of the dye-sensitized solar cell and silicon, and ensues that the spectral mismatch correction factor approaches unity. The voltage step and scan rate were 10 mV and 100 ms, respectively. A special black plastic mask with an aperture area of 5 $cm^2$ was covered on each testing cell during measurement to eliminate light reflection leading to unreliable results. Incident photo-current efficiency (IPCE) studies were carried out by means of Bentham PVE 300 analyzer, with xenon/quartz halogen light source and measured in DC mode with low chopping frequency (<1 Hz). The device was calibrated with reference photodiode DH Si. A cell spectral response was obtained at 25 °C for wavelengths range 300–800 nm with 5 nm step.

## 3. Results and discussion

### 3.1. Synthesis

The aim of this work was the development and photovoltaic characterization of new heteroleptic ruthenium complexes for DSSC application, containing **BDF** moiety combined with 2,2′-bipyridine as ligands and their comparison with commercially available **N719** and **Z907** dyes (Fig. 3). The heteroleptic complexes were prepared using ester form of **BDF** ligands and 2,2′-bipyridine-4,4′-dicarboxylic acid. Two alkyl esters, ethyl and 1-octyl, have been chosen to investigate the effect of the ester chain length on the solubility of dyes and efficiency of fabricated dye-sensitized solar cells based on these dyes.

The synthesis of **BDF** ligands started from ethyl and *n*-octyl 5-hydroxy-6-iodo-2-methylbenzofuran-3-carboxylates (**3**, **4**) obtained as shown in Scheme 1. Ethyl 5-hydroxy-2-methylbenzofuran-3-carboxylate (**1**) was prepared according to Bernatek and Ledaal [28] procedure from *p*-benzoquinone and ethyl acetylacetate in the presence of anhydrous zinc chloride in 43% yield. Acid catalyzed transesterification with 1-octanol led to octyl 5-hydroxy-2-methylbenzofuran-3-carboxylate (**2**) in 80% yield. Both **1** and **2** were iodinated by modified Giza and Hinman [27] protocol to give the desired products **3** and **4** in 34% and 52% yield respectively.

The **BDF** ligands **6a** and **6b** were prepared in the one-pot procedure involving the Sonogashira coupling reaction and palladium catalyzed cyclization leading to a new furan ring (Scheme 2). 4,4′-Dibromo-2,2′-bipyridine reaction with ethynyltrimethylsilane in the presence of 10% mol [1,1′-bis(diphenylphosphino)ferrocene] dichloropalladium(II) and copper iodide in toluene followed by cleavage of trimethylsilyl groups with tetrabutylammonium fluoride led to 4,4′-diethynyl-2,2′-bipyridine (**5**).

Addition of **3** or **4** to the reaction flask resulted in the second Sonogashira reaction followed by palladium catalyzed cyclization of hydroxyl group and triple bond to form a new furan ring in 78% and 96% yield, respectively. Unfortunately all attempts to hydrolyze the ester groups failed, mainly due to low solubility of both esters and acid in polar solvents.

The desired heteroleptic ruthenium complexes were prepared in one-pot process (Scheme 3). The **BDF** ligands were reacted with dichloro(*p*-cymene)ruthenium(II) dimer until all substrates were consumed, as judged by UV–Vis spectra (~2h). The resulting intermediate complexes were reacted with 2,2′-bipirydylo-4,4′-dicarboxylic acid and then with ammonium thiocyanate to replace chlorine atoms with isothiocyanate groups.

The reaction proceeds similarly when ruthenium(III) chloride is used as a source of ruthenium. Crude products were purified by column chromatography on Sephadex LH-20 with DMF as eluent. The main band was collected, and the process was repeated three times. Pure complexes were titrated in ethanol with tetrabutylammonium hydroxide solution to pH = 9 and then with 0.01M $HNO_3$ to pH = 5.2. The complexes (dyes) were obtained as black, shiny microcrystalline solids.

### 3.2. Spectroscopic properties of the dyes

The dyes **M43** and **M44** showed good solubility in ethanol and $1 \times 10^{-4}$ M solutions, required for dyeing process, were prepared. Their UV–Vis spectra in comparison with commercial **N719** and **Z907** (Fig. 4) were recorded at lower concentration ($5 \times 10^{-6}$ M) to achieve absorbance below 0.1 for low-energy CT band at ~530 nm and to avoid deviations from the Beer–Lambert law. The visible region band is typical for heteroleptic polypyridyl ruthenium(II) complexes [13,29].

The spectra revealed higher molar extinction coefficient of **M43** and **M44** for both LCCT (350–450 nm) and MLCT (500–600 nm) absorption bands in comparison to commercial dyes (Fig. 4). Although the low energy MLCT band for **M43** has almost the same molar absorption coefficient as **N719** ($\varepsilon$ = 13600 $M^{-1}$ $cm^{-1}$ vs. $\varepsilon$ = 13760 $M^{-1}$ $cm^{-1}$) the molar absorption coefficient for LCCT band is much higher ($\varepsilon$ = 23200 $M^{-1}$ $cm^{-1}$ vs. $\varepsilon$ = 16000 $M^{-1}$ $cm^{-1}$) (Table 1).

The **M44** dye revealed even higher molar absorption coefficient for both LCCT and MLCT bands than **M43**. The MLCT transition absorption for **M43** and **M44** peaks at 538 nm and 533 nm, respectively, are red-shifted compared to **Z907** (521 nm) and **N719** (526 nm).

The spectra of **M43** and **M44** solutions in ethanol, and anchored on a 5 μm thick transparent nanocrystalline $TiO_2$ film, have almost identical profiles (Fig. 5).

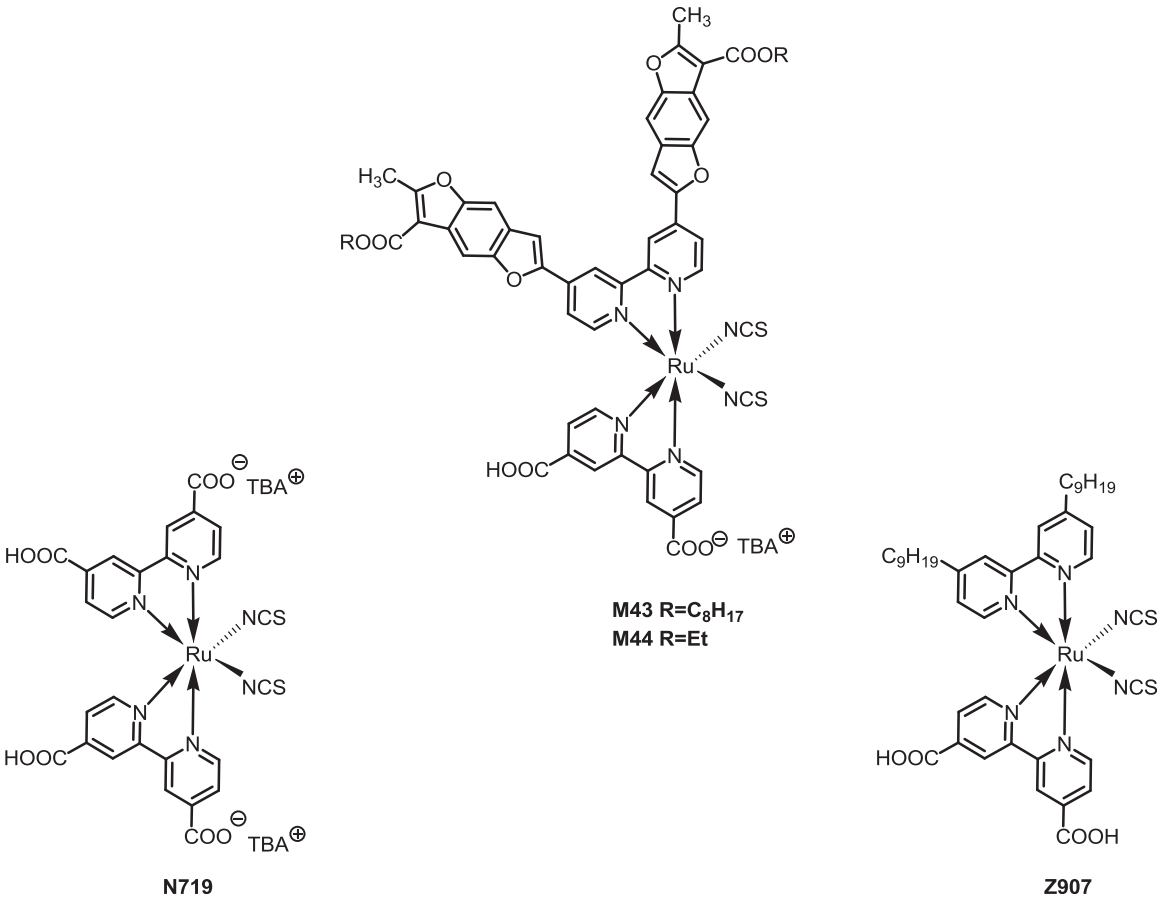


**Fig. 3.** Molecular structures of **N719**, **Z907**, **M43** and **M44.**

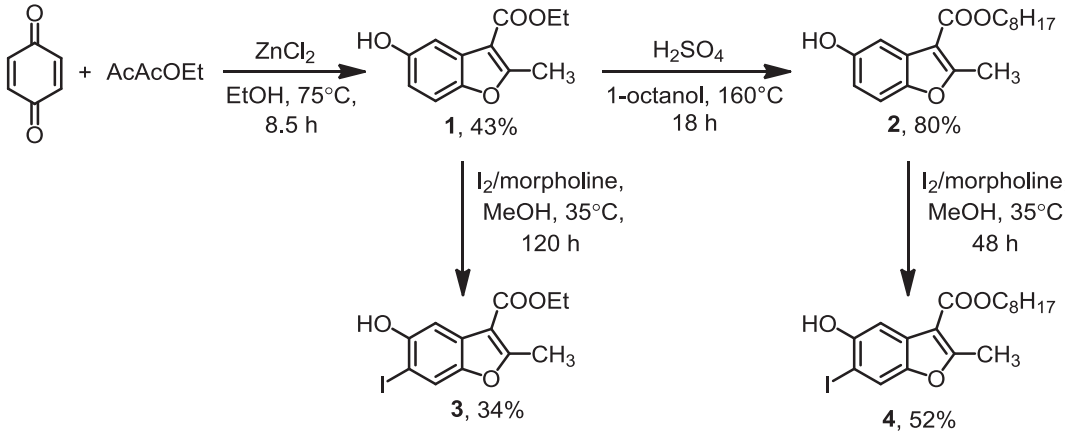


**Scheme 1.** Synthesis of 5-hydroxy-6-iodo-2-methylbenzofuran-3-carboxylates for the Sonogashira coupling.

### 3.3. Photovoltaic characterization

Two methods of dyeing test cells coated with a thin layer (5 μm) of titanium dioxide were examined – dip dyeing and flow dyeing. DSSC photovoltaic performances were used in order to compare these methods and applied dyes. For each cell, photovoltaic parameters such as: open-circuit voltage ($V_{oc}$), short-circuit current ($I_{sc}$), fill factor (FF), max power output ($P_m$), max power voltage ($V_m$), max power current ($I_m$), and solar-to-electric energy conversion efficiency ($\eta$) were determined. For each applied dye 48 cells were measured: 24 for dip dyeing and 24 for flow dyeing method. The obtained average results were summarized in Table 2. Moreover, Fig. 6 and Fig. 7 present current–voltage characteristics and spectral response as a function of wavelength for chosen cells, respectively.

As shown in Table 2, the short-circuit current ($I_{sc}$) of cells with newly synthetized **M44** and **M43** dyes is higher than with commercially available **N719** and **Z907** sensitizers, what corresponds to their higher efficiency and power. This tendency is visible for both dyeing methods. However, a significant difference

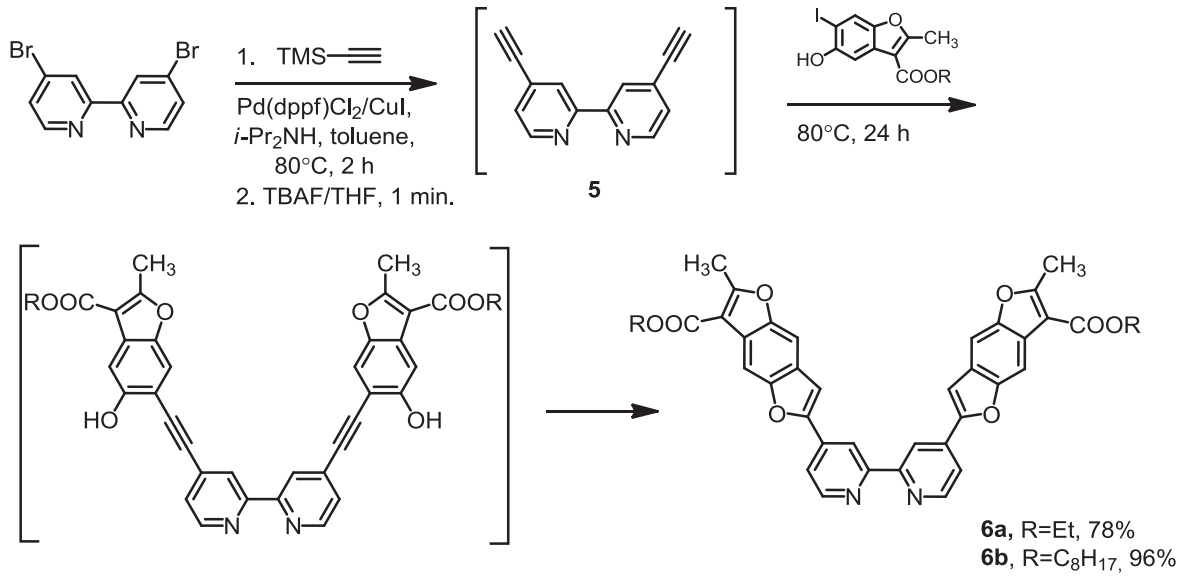


**Scheme 2.** The "one pot" synthesis of **BDF**-bipyridine ligands.

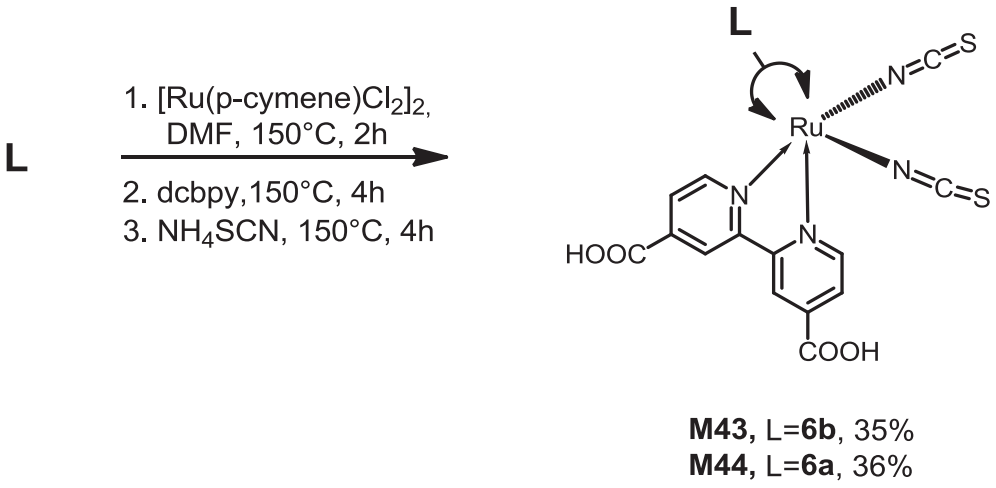


**Scheme 3.** Synthesis of heteroleptic **BDF**-bipyridine–dcbpy ruthenium(II) complexes.

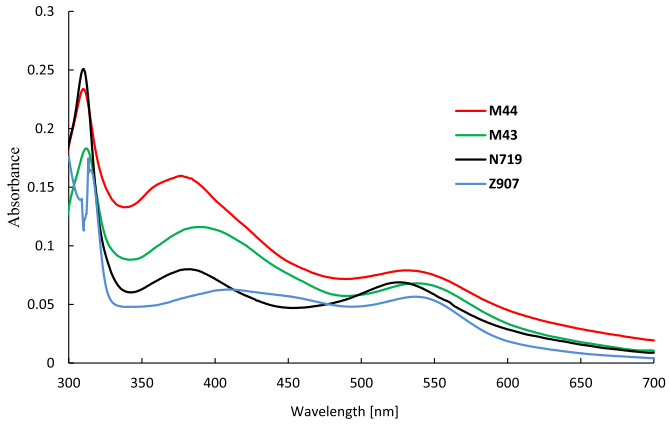


**Fig. 4.** Absorption spectra of **M43**, **M44**, **N719**, and **Z907** in ethanol.

**Table 1**
Molar absorption coefficients and wavelengths maxima for **M43**, **M44**, **N719**, and **Z907** in ethanol.

| Dye | LCCT ε [$M^{-1}$ $cm^{-1}$]/$\lambda_{max}$ [nm] | MLCT ε [$M^{-1}$ $cm^{-1}$]/$\lambda_{max}$ [nm] |
|---|---|---|
| **M43** | 23,200/391 | 13,600/538 |
| **M44** | 31,940/377 | 15,800/533 |
| **N719** | 16,000/382 | 13,760/526 |
| **Z907** | 12,534/411 | 6440/521 |

between these methods was noticed. Thus, considering the same photovoltaic parameters, the obtained values for the dip dyeing are lower than for the flow dyeing process, e.g. the cell with **M44** dye exhibits an increase in $I_{sc}$ and in $\eta$ from 29.7 mA to 32.7 mA and 2.56%–2.81%, respectively. This trend is also observed in incident photon-to-current efficiency (IPCE) plots. IPCE indicates the ratio of the number of photons incident on a solar cell to the number of

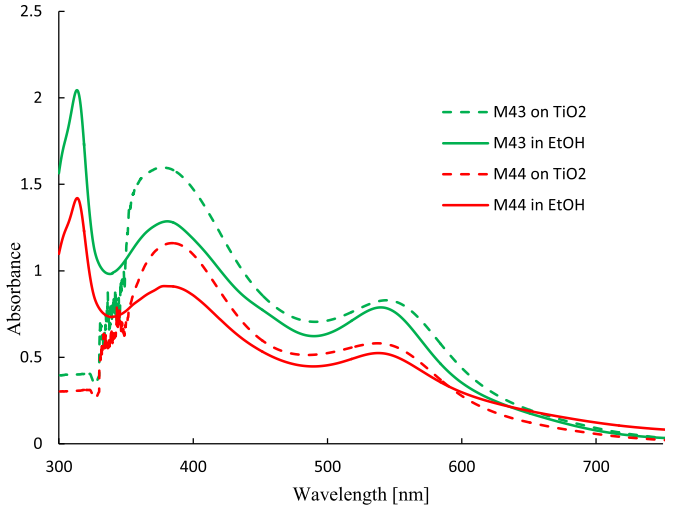


**Fig. 5.** Absorption spectra of **M43** and **M44** in ethanol and anchored on a 5 μm thick transparent nanocrystalline $TiO_2$ film.

**Table 2**
Average photovoltaic parameters of the dye-sensitized solar cells with different sensitizers for two dyeing methods.

| Complex | $V_{oc}$ [mV] | $I_{sc}$ [mA] | $V_m$ [mV] | $I_m$ [mA] | $P_m$ [mW] | FF | $\eta$ [%] |
|---|---|---|---|---|---|---|---|
| Dip dyeing | | | | | | | |
| **M43** | 664 | 29.2 | 479 | 26.5 | 12.7 | 0.66 | 2.54 |
| **M44** | 666 | 29.7 | 479 | 26.4 | 12.8 | 0.65 | 2.56 |
| **N719** | 679 | 24.2 | 511 | 22.2 | 11.3 | 0.69 | 2.26 |
| **Z907** | 742 | 19.1 | 529 | 17.0 | 8.91 | 0.64 | 1.75 |
| Flow dyeing | | | | | | | |
| **M43** | 662 | 28.8 | 479 | 26.2 | 12.5 | 0.66 | 2.51 |
| **M44** | 670 | 32.7 | 473 | 29.7 | 14.0 | 0.64 | 2.81 |
| **N719** | 671 | 25.5 | 495 | 23.5 | 11.6 | 0.68 | 2.32 |
| **Z907** | 764 | 21.2 | 550 | 19.0 | 10.5 | 0.65 | 2.06 |

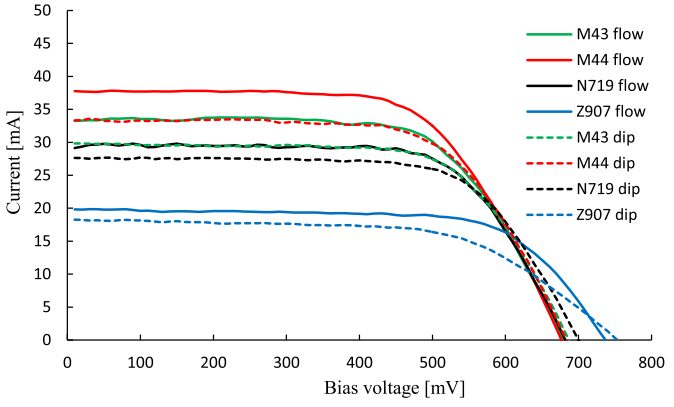


**Fig. 6.** Current – voltage characteristics of DSSC with **M43**, **M44**, **N719** and **Z907** sensitizers for two dyeing methods measured under illumination of AM1.5G sunlight (100 mW/cm$^2$). Aperture area of the testing mask: 5 cm$^2$.

generated charge carriers. The obtained results for devices with newly synthesized dyes show higher IPCE values in the wavelength range of 350–490 nm and 540–700 nm in comparison to **N719** and **Z907** dyes (Fig. 7). However, **N719** has slightly better performance than **M43** above 490 nm up to 540 nm, but worse than **M44**. The **M44** sensitizer has an advantage over the other studied dyes and achieves the highest IPCE values in the entire wavelength range. It was noticed that photovoltaic parameters strongly depend on the

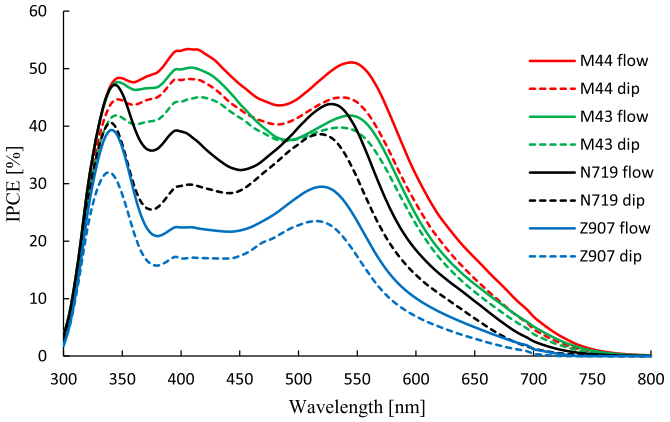


**Fig. 7.** Incident-photon-to-current conversion efficiency spectra of DSSC based on nanocrystalline $TiO_2$ film sensitized by **M43**, **M44**, **N719** and **Z907** dyes for two dyeing methods.

dyes absorption properties. Having compared Fig. 4 and Fig. 7 a good relationship was observed between behavior of the dyes in solution and in working DSSC device. The investigated dyes indicate the highest absorption in the spectral region from 350 to 560 nm which is correlated with the achieved IPCE values. To sum up, the evaluated DSSCs, based on nanocrystalline $TiO_2$ film sensitized by **M43**, **M44**, **N719** and **Z907** dyes for two dyeing methods, exhibit the same trend with the order **M44** > **M43** > **N719** > **Z907** for current–voltage characteristics and IPCE curves. However, the flowing process gives better photovoltaic parameters than the dipping process.

Moreover, the flow dyeing method has further advantages in comparison to dip dyeing process from practical point of view. Firstly, it does not need as much dye solution as the second method. Secondly, flow dyeing time is shorter than dip dyeing and takes only 8 h whereas dipping needs 24 h. Additionally, flow dyeing process is carried out in a closed system, without contact with moisturizing air, which may cause dyes degradation.

Its noteworthy that values of efficiency for cells sensitized by commercially available dyes are ~4 times smaller than reported in literature. This can be explained by the fact that we applied testing conditions more similar to the industrial ones. There was used much larger testing cell area (5 cm$^2$) than 0.158 cm$^2$ standard testing cell reported in the literature, and only single 5 μm transparent layer without scattering layer was used to maintain maximum transparency. The “green” solvent, ethanol, preferred in industrial applications was used. In these conditions our heteroleptic dyes revealed much higher efficiency than the most commonly used heteroleptic dye **Z907** (145% and 146% for **M43** and **M44**, respectively using dip dyeing, and 121% and 136%, respectively using flow dyeing process). Moreover, both newly synthesized dyes revealed also higher efficiency than the most commonly used homoleptic dye **N719** (112% and 113% for **M43** and **M44**, respectively using dip dyeing, and 108% and 121%, respectively using flow dyeing process). Assuming that the efficiency of 0.158 cm$^2$ standard testing cell sensitized with **N719** in laboratory conditions is 11.18% [6] using dip dyeing in 1:1 mixture of acetonitrile:*tert*-butanol, $c = 5 \times 10^{-4}$ M, we predict that **M43** and **M44** could achieve in these conditions efficiency of ~12.6%.

## 4. Conclusion

We report herein the design, synthesis, and characterization of novel heteroleptic ruthenium dyes **M43** and **M44** containing

benzodifuran moieties conjugated with the anchoring 2,2′-bipyridine group as a ligand. Both newly synthesized dyes revealed increased molar extinction coefficients compared with **Z907** and **N719** dyes in the visible light and the near-IR regions. Two dyeing methods, dip and flow dyeing, were used for the preparation of large area testing cells. The evaluated DSSCs based on nanocrystalline $TiO_2$ 5 μm transparent film, sensitized by **M43**, **M44**, **N719** and **Z907** dyes for two dyeing methods, exhibit the same trend with the order **M44** > **M43** > **N719** > **Z907** for current–voltage characteristics and IPCE curves, however, cells prepared in the flowing process revealed better photovoltaic parameters than prepared in dipping. The newly synthesized dyes revealed higher energy conversion efficiency ($\eta$), measured at the AM1.5G conditions, up to 21% compared to **N719** and up to 46% compared to **Z907**.

## Acknowledgments

We acknowledge financial support of this work by The National Centre for Research and Development, Warsaw, POIG.01.04.00-04-097/12 and POIG.01.04.00-18-101/12 Grants.

## References

[1] O'Regan B, Grätzel M. A low-cost, high-efficiency solar cell based on dye-sensitized colloidal TiO2 films. Nature 1991;353:737–40.
[2] http://www.nrel.gov/ncpv/images/efficiency_chart.jpg.
[3] Zhou H, Chen Q, Li G, Luo S, Song TB, Duan HS, et al. Interface engineering of highly efficient perovskite solar cells. Science 2014;345:542–6.
[4] Nazeeruddin MK, Kay A, Rodicio I, Humpbry-Baker R, Müller E, Liska P, et al. Conversion of light to electricity by cis-X2bis(2,2'-bipyridyl-4,4'-dicarboxylate)ruthenium(II) charge-transfer sensitizers (X = Cl-, Br-, I-, CN-, and SCN-) on nanocrystalline titanium dioxide electrodes. J Am Chem Soc 1993;115:6382–90.
[5] Nazeeruddin MK, Zakeeruddin SM, Humphry-Baker R, Jirousek M, Liska P, Vlachopoulos N, et al. Acid–base equilibria of (2,2'-bipyridyl-4,4'-dicarboxylic acid)ruthenium(II) complexes and the effect of protonation on charge-transfer sensitization of nanocrystalline titania. Inorg Chem 1999;38:6298–305.
[6] Nazeeruddin MK, De Angelis F, Fantacci S, Selloni A, Viscardi G, Liska P, et al. J Am Chem Soc 2005;127:16835–47.
[7] Wang Q, Ito S, Grätzel M, Fabregat-Santiago F, Mora-Sero I, Bisquert J, et al. Characteristics of high efficiency dye-sensitized solar cells. J Phys Chem B 2006;110:25210–21.
[8] Wang P, Zakeeruddin SM, Moser JE, Nazeeruddin MK, Sekiguchi T, Grätzel M. A stable quasi-solid-state dye-sensitized solar cell with an amphiphilic ruthenium sensitizer and polymer gel electrolyte. Nat Mater 2003;2:402–7.
[9] Wang P, Zakeeruddin SM, Comte P, Charvet R, Humphry-Baker R, Grätzel M. Enhance the performance of dye-sensitized solar cells by co-grafting amphiphilic sensitizer and hexadecylmalonic acid on $TiO_2$ nanocrystals. J Phys Chem B 2003;107:14336–41.
[10] Zakeeruddin SM, Nazeeruddin MK, Humphry-Baker R, Pechy P, Quagliotto P, Barolo C, et al. Design, synthesis, and application of amphiphilic ruthenium polypyridyl photosensitizers in solar cells based on nanocrystalline $TiO_2$ Films. Langmuir 2002;18:952–4.
[11] Chen CY, Wu SJ, Wu CG, Chen JG, Ho KC. A ruthenium complex with superhigh light-harvesting capacity for dye-sensitized solar cells. Angew Chem Int Ed 2006;45:5822–5.
[12] Chen CY, Chen JG, Wu SJ, Li JY, Wu CG, Ho KC. Multifunctionalized ruthenium-based supersensitizers for highly efficient dye-sensitized solar cells. Angew Chem Int Ed 2008;47:7342–5.
[13] Gao F, Wang Y, Shi D, Zhang J, Wang M, Jing X, et al. Enhance the optical absorptivity of nanocrystalline $TiO_2$ film with high molar extinction coefficient ruthenium sensitizers for high performance dye-sensitized solar cells. J Am Chem Soc 2008;130:10720–8.
[14] Gao F, Wang Y, Zhang J, Shi D, Wang M, HumphryBaker R, et al. Chem Commun 2008:2635–7.
[15] Nazeeruddin MK, Bessho T, Cevey L, Ito S, Klein C, De Angelis F, et al. A high molar extinction coefficient charge transfer sensitizer and its application in dye-sensitized solar cell. J Photoch Photobio A 2007;185:331–7.
[16] Gao F, Cheng Y, Yu Q, Liu S, Shi D, Li Y, et al. Conjugation of selenophene with bipyridine for a high molar extinction coefficient sensitizer in dye-sensitized solar cells. Inorg Chem 2009;48:2664–9.
[17] Jang SR, Yum JH, Klein C, Kim KJ, Wagner P, Officer D, et al. High molar extinction coefficient ruthenium sensitizers for thin film dye-sensitized solar cells. J Phys Chem C 2009;113:1998–2003.
[18] Chen CY, Wang M, Li JY, Pootrakulchote N, Alibabaei L, Ngocle CH, et al. Highly efficient light-harvesting ruthenium sensitizer for thin-film dye-sensitized solar cells. ACS Nano 2009;3:3103–9.
[19] Cao Y, Bai Y, Yu Q, Cheng Y, Liu S, Shi D, et al. Dye-sensitized solar cells with a high absorptivity ruthenium sensitizer featuring a 2-(hexylthio)thiophene conjugated bipyridine. J Phys Chem C 2009;113:6290–7.
[20] Yu Q, Liu S, Zhang M, Cai N, Wang Y, Wang P. An extremely high molar extinction coefficient ruthenium sensitizer in dye-sensitized solar cells: the effects of π-conjugation extension. J Phys Chem C 2009;113:14559–66.
[21] Kim JJ, Choi H, Kim C, Kang MS, Kang HS, Ko J. Novel amphiphilic ruthenium sensitizer with hydrophobic thiophene or thieno(3,2-b)thiophene-substituted 2,2′-dipyridylamine ligands for effective nanocrystalline dye sensitized solar cells. Chem Mater 2009;21:5719–26.
[22] Yu Q, Wang Y, Yi Z, Zu N, Zhang J, Zhang M, et al. High-efficiency dye-sensitized solar cells: the influence of lithium ions on exciton dissociation, charge recombination, and surface states. ACS Nano 2010;4:6032–8.
[23] Yen YS, Chen YC, Hsu YC, Chou HH, Lin JT, Yin DJ. Heteroleptic ruthenium sensitizers that contain an ancillary bipyridine ligand tethered with hydrocarbon chains for efficient dye-sensitized solar cells. Chem Eur J 2011;17:6781–8.
[24] Chandrasekharam M, Rajkumar G, Srinivasa Rao C, Suresh T, Reddy PY, Soujanya Y. Ruthenium(II)- bipyridyl with extended π-system: improved thermo-stable sensitizer for efficient and long-term durable dye sensitized solar cells. J Chem Sci 2011;123:555–65.
[25] Huang WK, Wu HP, Lin PL, Diau EWG. Design and characterization of heteroleptic ruthenium complexes containing benzimidazole ligands for dye-sensitized solar cells: the effect of thiophene and alkyl substituents on photovoltaic performance. J Phys Chem C 2013;117:2059–65.
[26] Ciana LD, Dressick WJ, Von Zelewsky A. Synthesis of 4,4′-divinyl-2,2′-bipyridine. J Heterocycl Chem 1990;27:163–5.
[27] Giza CA, Hinman RL. New thyroxine analogs. Halogen derivatives of 3-carbethoxy-5-hydroxy-2-methylbenzofuran. J Org Chem 1964;29:1453–61.
[28] Bernatek B, Ledaal T. The reaction between p-benzoquinone and ethyl acetoacetate. Acta Chem Scand 1958;12:2053–4.
[29] Wang P, Zakeeruddin SM, Moser JE, Humphry-Baker R, Comte P, Aranyos V, et al. Stable new sensitizer with improved light harvesting for nanocrystalline dye-sensitized solar cells. Adv Mater 2004;16:1806–11.